

Rift assessment and potential calving zone of Amery Ice Shelf, East Antarctica

Simone Darji^{1,*}, Sandip R. Oza², R. D. Shah¹,
B. P. Rathore² and I. M. Bahuguna²

¹Geology Department, M.G. Science Institute, Navrangpura, Ahmedabad 380 009, India

²Space Applications Centre, ISRO, Jodhpura Tekra, Ahmedabad 380 015, India

Ice shelves line the peripheries of Antarctica. Rift and crevasses are two main deformational structures affecting ice shelf stability. The present study deals with propagation-widening of five active rifts and future potential calving zones on Amery Ice Shelf (AIS), East Antarctica, between 2000 and 2017 using moderate resolution image spectroradiometer (MODIS) data. The widening and rift propagating rate, as well as advancement in AIS show abnormal behaviour. The expansion of AIS differs across the shelf. The highest rate of advancement was observed in 2012–2013 (~517 sq. km) and the lowest was observed in 2000–2001 (~35 sq. km). The rift system shows variability in its proportion and having poor relationship with environmental processes, which suggests heterogeneities in the AIS. The abnormal behaviour of rift propagation during the study period can be attributed to tsunamis, tide, current action, crevasses pattern and icequakes in the vicinity of the study region.

Keywords: Amery Ice Shelf–Lambert glacier system, rift system, potential calving zone.

BASAL melting and iceberg calving are the two main processes involved in elimination of ice mass from the Antarctic Ice sheet. Amery Ice Shelf (AIS)–Lambert Glacier system has an area of about 1,380,000 sq. km through a section of coastline ideal to study, and is a sensitive indicator for change in the global climate system^{1,2}. Mass loss from the Antarctica ice sheet takes place at its ice shelves and outlet glaciers². Antarctica ice shelves experience a large number of calving events, where significant sections break away as tabular or irregular icebergs, following decades of rift propagation in the ice shelf^{2–4}. Rifts are considered the most unstable part of ice shelves that cut-through crevasses, which are cracks on the surface. When the cracks deepen, they are called rifts. The rift is a large fracture that propagates transverse to the ice flow direction and acts as a precursor to ice calving. Rift propagation and iceberg calving are natural phenomena at Antarctic ice margins. In the Antarctica peninsula, rift propagation is attributed to global warming. As the temperature increases, ice melts and percolates through crevasses/rift and reaches the ocean. This

process hastens rifting and eventually leads to icebergs⁵. However, the impact of environmental stresses on rift propagation is negligible^{2,6}. Rifting is an important glaciological process. It is important to monitor these rifts, as it is the weaker portion for future calving, which could eventually lead to icebergs and global sea level rise. Ocean circulation generates varying stress underneath the ice shelf⁶. Understanding rift mechanisms, monitoring them, and studying its evolution are critical to quantifying the mass balance⁸.

The present study focuses on propagation of five active rifts in AIS, in terms of its widening, lengthening and frontal advancement. The study of spatial and temporal variation of AIS was carried out for rift assessment, advancement and possible impacts.

AIS comprises three main giant tributary glaciers – Lambert, Mellor and Fisher – having a surface area of ~64,000 sq. km (refs 2, 9), floating on Prydz Bay between Mac Robertson Land and Prince Elizabeth Land (Figure 1).

Our aim was to monitor the active rifts of AIS. The associated active rifts system (Figure 2) consists of two longitudinal-to-flow rifts (L4 and L3) and two transverse-to-flow rifts (T1 and T2). T1 and T2 propagate in west and east direction respectively. These rifts are initiated from the tip of L4, forming triple junction (V). Both T1 and T2 were initiated in the transition zone where transverse-to-flow strain rate exceeds longitudinal-to-flow strain rates^{10,11}.

Rifts L5, L6 and T2 are east propagating whereas L1, L2, L3 and T1 rifts are west propagating (Figure 2). The behaviour of rifts is generally categorized as dormant and active based on recurrence character between rift propagation events. Rifts that did not propagate over decades are defined as dormant (<~500 m over the decades), e.g. L3 rift. Rifts that open up repetitively are termed active (~500 m over decades); such rifts are further, subdivided into. (i) Continuously active rifts that propagate continuously, e.g. rift L4, (ii) intermittently active rifts, appears to propagate continuously for two or more years before becoming dormant for a decade and (iii) sudden burst active rifts, which exhibited propagation events larger than ~500 m after two or more years of dormancy, e.g. rift T1 (ref. 12).

MODIS (optical) and SENTINEL-1B and RADARSAT-I & II (microwave) data were used to monitor the rift system. Low spatial but high temporal resolution MODIS cloud-free data (Table 1) of summer (January to early March) was utilized for monitoring. RADARSAT-I & II data were used to compare the MODIS derived results for 1997 and 2008. RADARSAT-I and RADARSAT-II are C-band (5.3 and 5.45 GHz) Synthetic Aperture Radar (SAR) with a 500 km swath. Ground range detected geo-referenced products of C-band SENTINEL-1B SAR data (Table 1) having an extra wide swath of 400 km for February was used for study.

*For correspondence. (e-mail: dsimone24@gmail.com)

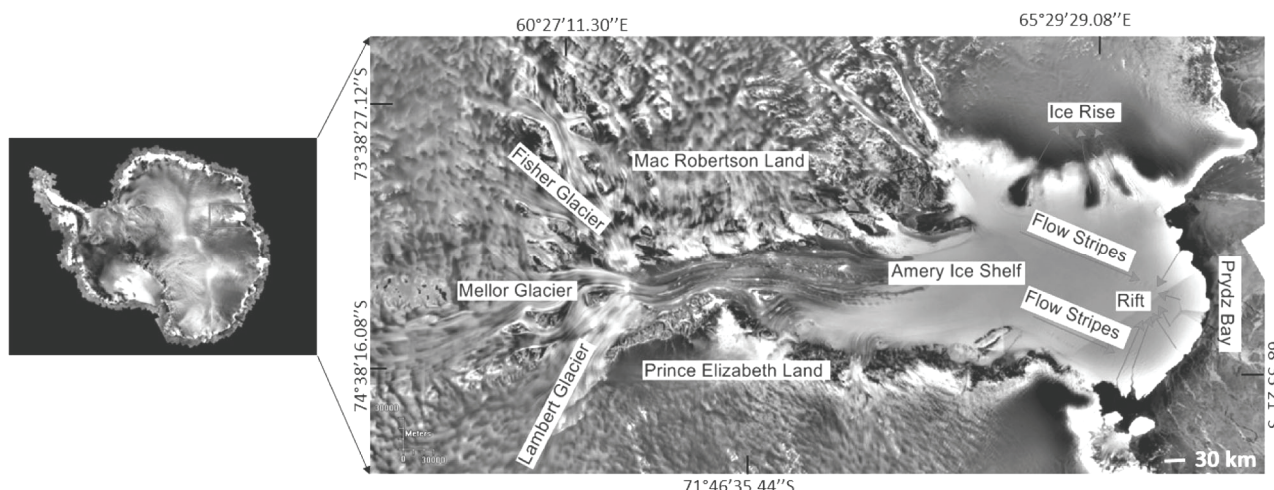


Figure 1. Location map of Amery Ice Shelf (AIS), East Antarctica (Radarsat II) (modified after Chen *et al.*).

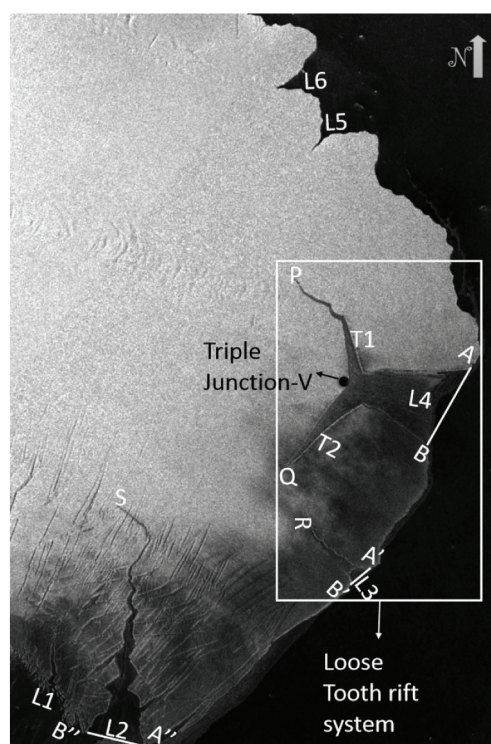


Figure 2. Image showing the location of the rift acquired on 8 February 2017 (Sentinel – 1B) showing eight rifts (L1, L2, L3, L4, L5, L6, T1 and T2), three major lateral rift (L2, L3 and L4) and two major transverse rift (T1 and T2).

Table 1. Information of sensors with its acquisition and its resolution

Sensors	Year of acquisition	Resolution of data
MODIS	2000–2017	250 m
SENTINEL-1B	2017 February	25 × 100 m (HH-Pol)
RADARSAT-I	1997	125 m
RADARSAT-II	2008	100 m (HH-Pol)

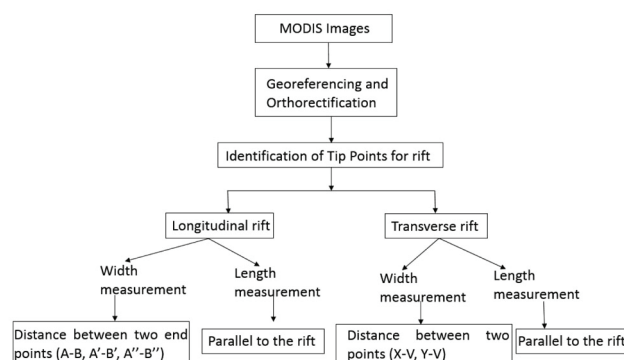


Figure 3. Flow chart of methodology.

Widening and lengthening of rift and advancement of frontal portion of AIS was measured using MODIS data from 2000 to 2017; patterns of rift and prediction of potential zone were identified using SENTINEL-1B data (Figure 2), whereas RADARSAT-I and -II data were used to add facts in the information. MODIS image was used for rift assessment and studying the advancement of the frontal portion AIS between 2000 and 2017. ERDAS imaging, version 2015, was used for pre-processing digital images. RADARSAT and Sentinel data were co-registered with each other. The measuring toolbox inbuilt in software was then used to calculate rift dimensions as shown in the flow diagram (Figure 3). To calculate the width of three longitudinal rifts, L4, L3 and L2 were measured by two end points like A–B, A'–B' and A''–B'' (Figure 2) respectively. However, triple junction V, with respect to R and S (Figure 2) was used to calculate rift length. To measure the width of two transverse rifts, triple junction V and points X and Y (Figure 2) were considered. The length was measured from triple junction point V with point P and Q respectively. Measuring tools from the image processing software were used to calculate rift

dimensions. This method can provide a systematic way to observed lengthening and widening of the rift over time.

The advancement of AIS shows non-uniform distribution (Figure 4) during the study period. The maximum advancement of ~ 517 sq. km was observed during 2012–13 and minimum advancement of ~ 35 sq. km was observed in 2000–2001, with a total advancement of ~ 3464 sq. km. During 2005/06, 2007/08, 2012/13 and 2014/15 (Figure 5), a high rate of expansion was observed compared to other study years. Uneven expansion of an area perceived in the study region (Figure 4) indicates abnormalities underneath the shelf. Various processes that accelerate the flow of ice added mass into

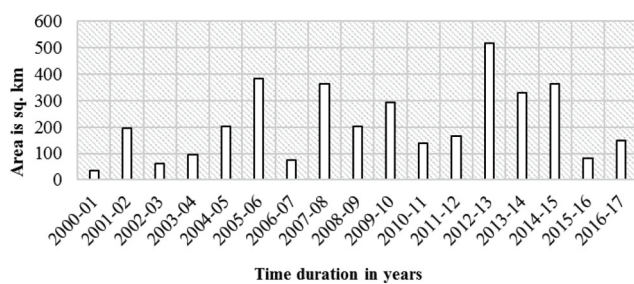


Figure 4. Annual advancement in the frontal portion of AIS between 2000/01 and 2016/17, maximum increment observed in 2013, whereas minimum increment observed in year 2001 followed by 2003/04/07/16.

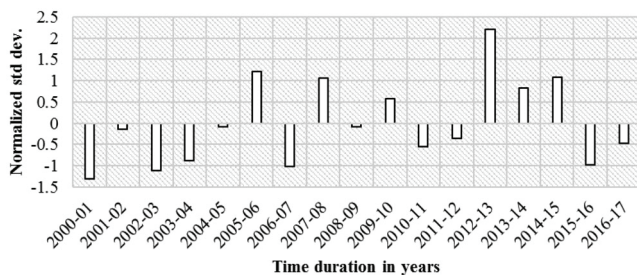


Figure 5. Normalized standard deviation in advancement of frontal area of AIS, positive bar in the year shows the advancement perceived by environmental forces.

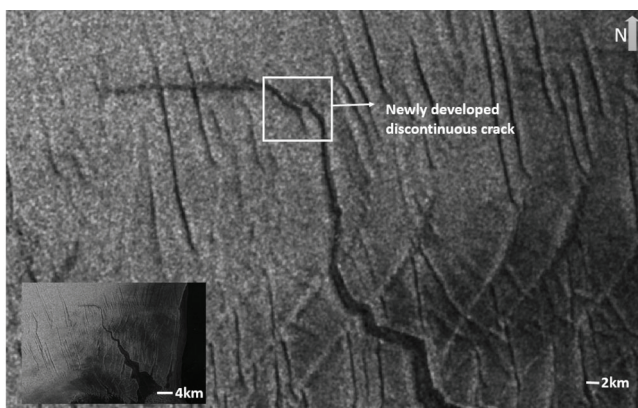


Figure 6. Freshly developed rift along the existing 'Jump'.

the ice shelf, which led to expansion of the frontal portion. Approximately, 3646 sq. km of area had advanced between 1997 and 2017. Errors could be in order of one MODIS pixel (250 m). The ice flow across an ice shelf velocity usually increases from grounding zone to the edge of the ice shelf, leading to frontal advancement independent of ice depth¹³. The advancement of AIS shows heterogeneity, which could be due to differences in ice velocity and ice flow direction. Moreover, the climatic condition, circumpolar currents, tsunami waves and oceanic waves are other reasons for heterogeneity.

From a total of eight active rifts, results for five rifts (L2, L3, L4, T1 and T2) were discussed in detail. Three rifts are prone to frequent change (L2, L3 and L4), as they are open to the ocean. It was observed that the pattern of rift lengthening and widening varied from rift to rift. Rift propagation is an episodic event and might be triggered by short timescale environmental forces like tides, winds and ocean swell, etc. and by other geophysical processes like earthquake and tsunamis¹¹. Rate of propagation also depends on seasonal variation. Rift propagate faster in summer than in winter, as the rate of melting is greater in summer⁷. Rate of propagation also varies with rift characteristics changes in shelf geometry due to internal glaciological stress² and interaction with crevasses¹² that serves rift propagation and widening. Temporal variability in rift propagation was dominant by large occasional bursts; they were not synchronous across rifts. Several propagation events took place after the predicted arrival from tsunamis originated in the Indian Ocean¹². High tides induce high velocity¹⁴ tsunamis, which leads to higher amplitude tidal waves that increase inflow of ice from glacier to the ice shelf. Moreover, due to bathymetric and geographic location, all tsunamis affect AIS¹⁵.

Average rate of propagation, observed on rifts T1 and T2 were ~ 3.64 and ~ 2.64 m/day, which were ~ 4.2 and ~ 2.1 m/day observed by Walker *et al.*². However, this difference is due to two main reasons. First they measured till 2014, while we have computed till 2017 and secondly, in recent years, the scenario has changed. T2 rift propagates with a higher rate than T1. The detached block of an area ~ 195.6 sq. km moved 23 km towards AIS, which might be due to an earthquake of 7.3 magnitude observed at South Bristol Island in South Sandwich Islands, that affects the rate of propagation, and widening of rift L2 (ref. 16). Minor fluctuation observed might be due to environmental forces like tides, winds, ocean swell that affects the rift^{11,17}. The detached crack highlighted in Figure 6 will join with pre-existing rift, forming one continuous elongated rift.

Rift L4 is an active longitudinal-to-flow rift in AIS system. Almost stable lengthening observed until 2017 (Figure 7). Gentle increase in widening (Figure 8) was observed for 10 consecutive years (1997 and 2007). A raise of ~ 4 km was seen in 2007 and steep growth of

~1.4 km in 2012. The average rate of lengthening and widening of L4 observed was ~5.1 and ~19 m/day respectively.

Rift L2, one of the most fascinating oblique-to-flow rifts, penetrating in the western direction (Figure 2) follows the zigzag pattern of crevasses. Observed lengthening of rift L2 was more than its widening, as it keeps propagating in the direction of pre-existing ruptures in its vicinity. Rift L2 opened up at the eastern part of the ice front before 1996 (ref. 2). The iceberg separated from Polar Times glacier tries to fit in the ‘V’ shaped L2 rift in between A”-B” (Figure 2)¹⁶. The combined effect of forces by large iceberg, wind and current along with other environmental forces could be acting on the progression of the rift. Gentle widening of ~12.8 km was observed between 1997 and 2017 (Figure 8). It shows maximum lengthening among all the rifts present in the system, i.e. ~56.55 km (Figure 7) in the direction of the flow stripes.

Since the last two-decades L3, was nearly stable; marking its dormancy. However, named under one of the major active rifts of AIS, it remains almost steady in its growth. That is a significant oddity of the rift. The observed lengthening and widening were ~700 and ~500 m respectively, since 1997 (Figures 7 and 8). Average rate of widening and lengthening observed at rift L3 was same, ~0.087 m/day that seems it is affected by environmental forces.

Rift T2 was considered one of the most active rifts in the beginning of its evolution. The crack in L2 gave birth to rift T1 and T2. T2 was more prone to environmental forces than T1 in the beginning, hence it pierced very fast compared to T1. Both in lengthening as well as widening T2 shows gradual growth. During 2007 a sudden rise in width (Figure 8) of the rift was observed, whereas in 2000, a sudden rise in lengthening was observed (Figure 7). The average rate of lengthening and widening was ~0.96 and ~0.24 km/year respectively.

Rift T1 is the most promising rift and combined with rifts L4 and T2, it forms a ‘loose-tooth’. Based on the study carried out using multitemporal data, it was observed that initially the rift was perpendicular to L4 until 2011. Subsequently, it became parallel to the rift that follows the direction of flow stripes (Figure 2).

Sudden rise in the width of L4 and T2 was witnessed in 2007 after the Sumatra island earthquake (<http://earthquake.usgs.gov/>) (Figure 8). Abrupt increase in width of rift L4 in 2012 after 8.6 magnitude earthquake was observed at Wharton Basin. Episodic propagation exploited by earthquake mechanics, surface melting has also an impact on rift propagation¹⁷. The tide fluctuations were also evident from mapping of Amery ice shelf grounding line using ICES at repeat-track¹⁹.

Rifts on the ice shelf are considered weaker zones for calving and disintegration into icebergs. Intersection of frontal longitudinal and transverse rift is one of the major causes for potential calving. All active rifts have potential

to calve the large masses of icebergs, creating uneven mass balance distribution. The AIS front is unequally distributed (Figure 9 a), T1 side shows more encroachment toward sea compared to T2 side, which was initiated in 2012 but was clearly observed in 2014 (Figure 9 c and d). The uneven growth of the frontal portion needs further investigation. After 2012, both the rifts show reverse effects, T1 rift shows increasing trend and T2 remains less functional since 2010.

The rifts present on AIS influence some future potential calving regions. The peripheral rift present in ice shelf joint together, eventually release huge chunk of ice, which will contribute to the sea level rise. Rifts T1, T2 and L3 are the controlling factor for calving of the ‘loose-tooth system’ (Q, P and P’) which in total has capability to calve ~2639 sq. km (Figure 9 b). However, since the last few years the condition has changed, where T2 has become more stable than rift T1 (Figure 10), demoting the probabilities of breaking ‘loose-tooth’ and intensifying the chances of separating L6-T1/L5-T1 (P and P’) more (Figure 9 b). The approximate size of possible ice chunk that separates from L6-T1 (P’) and L5-T1 (P) might be ~1797 and ~1518 sq. km respectively. The other calving zone controlled by rifts L1 and L2 (Figure 11) has potential to calve an area around ~340 sq. km (R and R’). The melting and back freezing of the snow-filled rift becomes

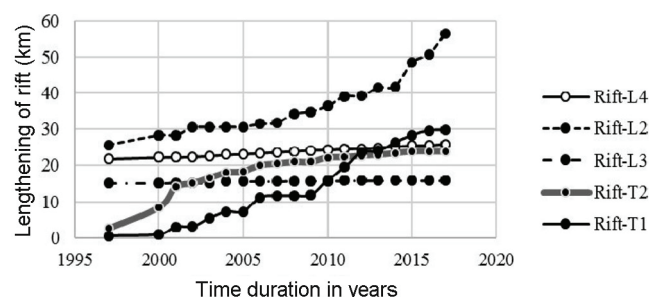


Figure 7. Lengthening of five active rifts of AIS shows that rifts L2 and T1 are most active, whereas rifts L3 and L4 increase very deliberately and rift T2 is intermediary in nature.

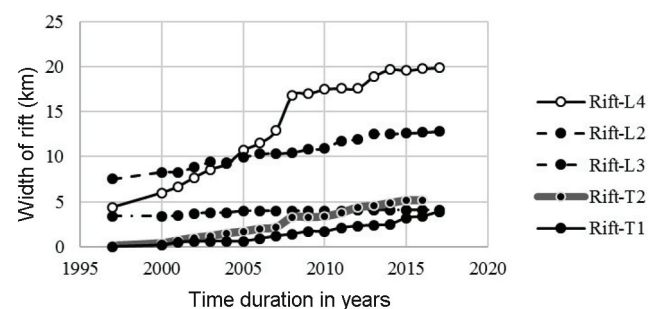


Figure 8. Widening of five active rifts of AIS shows that rifts T1, T2 and L2 increased gradually, whereas rift L4 shows abrupt growth in 2007 and then increases gradually and rift L3 is almost steady during these years.

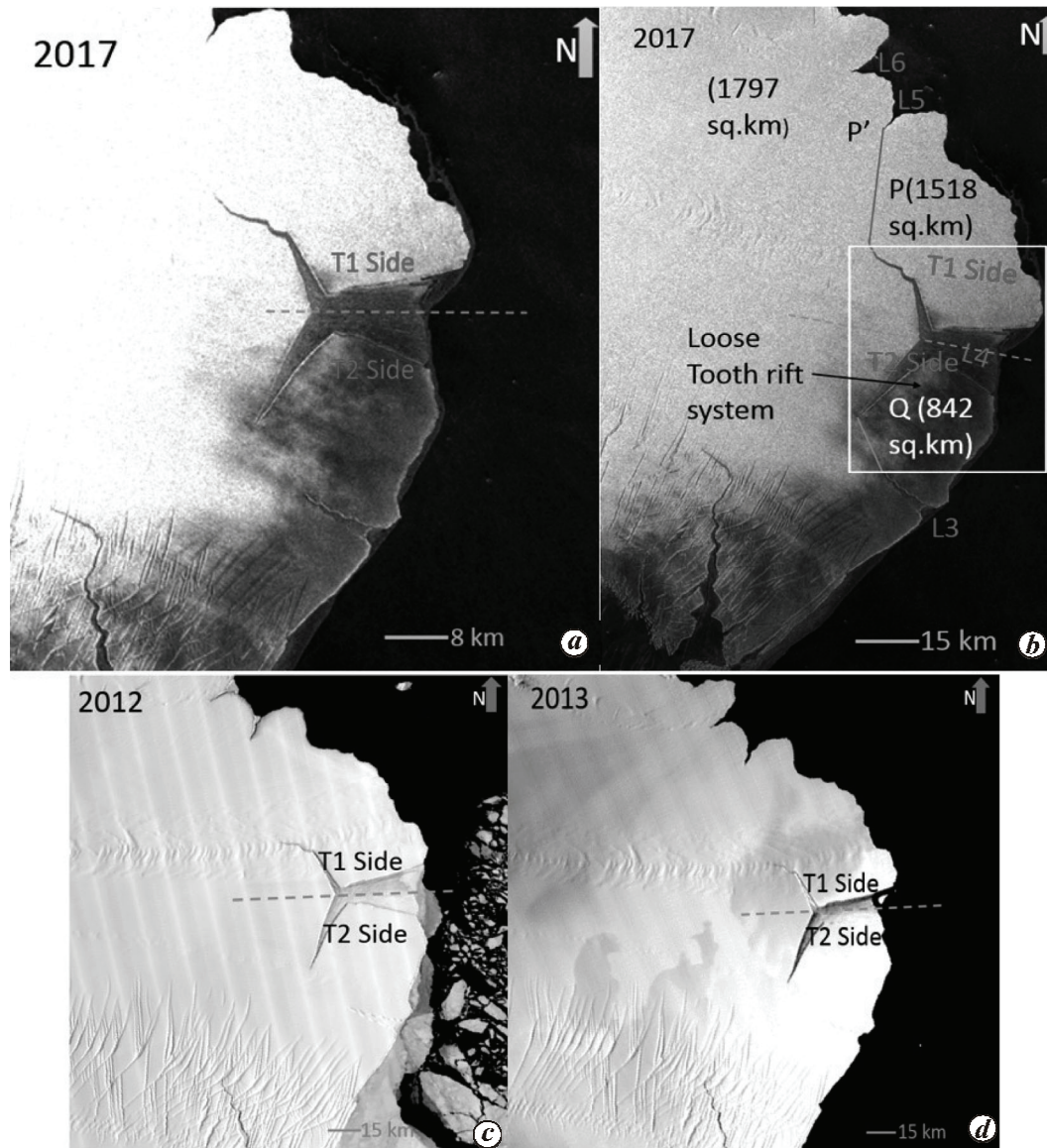


Figure 9. Image showing leading calving zone: *a*, rift T1 shows more advancement than rift T2; *b*, progression of cracks may lead to disintegration of icebergs from rift T1 and T2 using Sentinel-1B; *c*, *d*, MODIS image of 2012 and 2013 shows very slight and major changes in rifts T1 and T2 side.

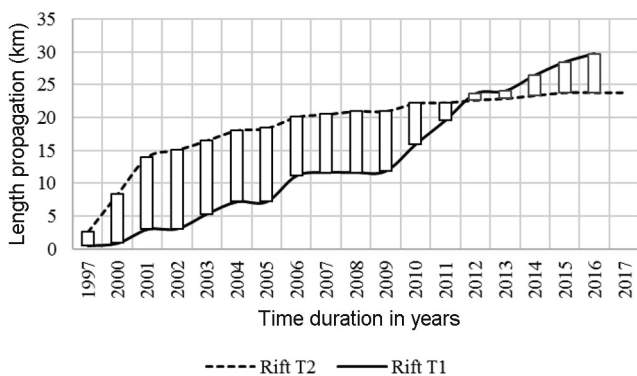


Figure 10. Progressive growth of rifts T1 and T2 with respect to each other, rift T1 shows sudden growth from 2009.

prime for rifting, helping crevasses to form a rift. Oblique-to-flow L2 rift shows distinct zigzag pattern and its breaking follows the same identical path. Recently developed L1 and L2 rifts are capable of separating 100 sq. km (*R'*) and ~240 sq. km (*R*) (Figure 11). Basal melting, bathymetry of the ice shelf, ocean-currents interaction and tidal effects are some of the controlling parameters for potential calving. The 'loose tooth' includes two longitudinal-to-flow rifts (L4 and L3) and two transverse-to-flow rifts (T1 and T2) with an area of 30 sq. km. The fracture will widen as the 'loose tooth' progressively separates from the main ice shelf⁸. The calving of 'loose tooth' was ~800 sq. km calculated from the tip with minimum aerial distance, detached in the form of tabular

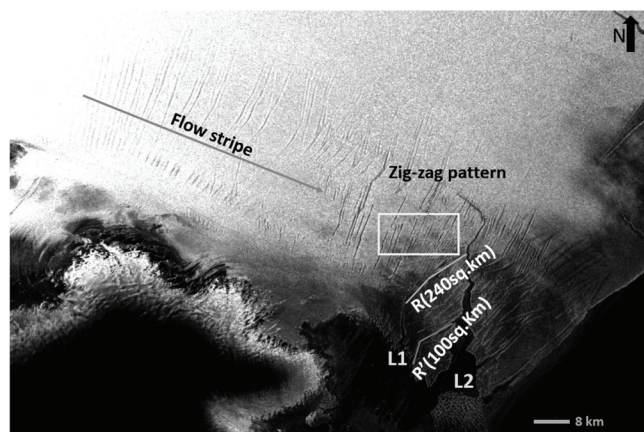


Figure 11. Prediction for calving of icebergs near active rift T2 (R and R').

icebergs¹⁸. The difference observed could be due to the fact that majority researchers have highlighted only one potential calving zone, whereas in the present study, we have discussed all potential calving zones.

Total advancement of AIS observed in the study area during 1997 to 2017 was ~3646 sq. km, the maximum rate of advancement was observed in 2012. The observation confirms that the rifts of AIS were prone to propagation and widening. All the rifts were active except rift L3. It was found that rifts L4 and L2 situated in the frontal have rapid rift widening events due to earthquakes and tsunamis. Expansion of frontal position of AIS was noted due to seismic activity taking place in the Indian Ocean. There were three major potential calving zones. The 'loose-tooth' formed from the tip of rifts L2 and T2 combined with rift L3 indicates the future calving zone which will detach ~842 sq. km area from the mass body. Similarly, other rifts like L4 and T1 combined with L5 or L6 will be able to calve ~1518 or ~1797s sq. km area. The processes of AIS advancement and calving contributes to global sea level rise. The study reveals many potential calving zone, which will affect the global sea level rise and mass balance. In future, it may be possible to connect all the environmental and seismic events with internal forces that are working beneath the shelf.

1. Bassis, J., Coleman, R., Fricker, H. and Minster, J., *Australian Antarctic Division: Leading Australia's Antarctic Program*, 2003; www.AustralianAntarcticDivision.com
2. Walker, C., Bassis, J., Fricker, H. and Czerwinski, R., Observation of interannual and spatial variability in rift propagation in the Amery Ice Shelf, Antarctica, 2002–14. *J. Glaciol.*, 2015, **61**(226), 243–252.
3. Jacobs, S., MacAyeal, D. and Ardal, J., The recent advance of the Ross Ice Shelf, Antarctica. *J. Glaciol.*, 1986, **32**(112), 464–474.
4. Lazzara, M., Jezek, K., Scambos, T., MacAyeal, D. and Van der Veen, C., On the recent calving of icebergs from the Ross Ice Shelf. *Polar Geography*, 1999, **23**(3), 201–212.
5. Jayaprasad, P., Ahmed, T., Maity, S. and Misra, A., Breaking of Larsen C from Antarctica. *Curr. Sci.*, 2018, **114**(5), 961–962.

6. Bassis, J., Fricker, H., Coleman, R. and Minster, J., An investigation into the forces that drive ice-shelf rift propagation on the Amery Ice Shelf, East Antarctica. *J. Glaciol.*, 2008, **54**(184), 17–27; doi:10.3189/002214308784409116.
7. Fricker, H., Young, N., Coleman, R., Bassis, J. and Minster, J., Multi-year monitoring of rift propagation on the Amery Ice Shelf. *Geophys. Res. Lett.*, 2005, **32**; doi:10.1029/2004GL021036.
8. Bassis, J., Coleman, R., Fricker, H. and Minster, J., Episodic propagation of a rift on the Amery Ice Shelf, East Antarctica. *Geophys. Res. Lett.*, 2005, **32**; doi:10.1029/2004GL022048.
9. Griggs, J. and Bamber, J., Antarctica ice-shelf thickness from satellite radar altimetry. *J. Glaciol.*, 2011, **57**(203), 485–498.
10. Budd, W., The dynamics of Amery Ice Shelf. *J. Glaciol.*, 1966, 335–358.
11. Bassis, J., Fricker, H., Coleman, R., Bock, Y., Behrens, J., Darnell, D. and Minster, J., Seismicity and deformation associated with ice-shelf rift propagation. *J. Glaciol.*, 2007, **53**, 523–536.
12. Walker, C., Bassis, J., Fricker, H. and Czerwinski, R., Structural and environmental controls on Antarctic ice shelf rift propagation inferred from satellite monitoring. *Geophys. Res. Lett.*, 2013, **118**(4), 2354–2364; doi:10.1002/2013jf002742.
13. Pittard, M. L., Roberts, J. L., Warner, R. C., Galton-Fenzi, B. K., Watson, C. S. and Coleman, R., Flow of the Amery Ice Shelf and its tributary glaciers. In 18th Australasian Fluid Mechanics Conference, Launceston, Australia, 2012.
14. Voytenko, D., Stern, A., Holland, D., Dixon, T., Christianson, K. and Walker, R., Tidally driven ice speed variation at Helheim Glacier, Greenland, observed with terrestrial radar interferometry. *J. Glaciol.*, 2015, **61**(226), 301–308.
15. Diandong, R. and Lance, L., Effects of Waves on Tabular Ice-Shelf Calving. *Earth Interact.*, 2014, **18**.
16. Jayaprasad, P., Rajak, D., Singh, R., Oza, S., Sharma, R. and Sharma, R., Ice calving and deformation from Antarctica ice margins using RISAT-1 circular polarized SAR data. *The International Archives of the Photogrammetry, Remote Sensing and Spatial Information Sciences*, XL-8, 2014.
17. Larour, E., Rignot, E. and Aubry, D., Modelling of rift propagation on Ronne Ice Shelf, Antarctica, and sensitivity to climate change. *Geophys. Res. Lett.*, 2004, **31**(16); doi:10.1029/2004GL020077.
18. Oza, S., Spatial-temporal patterns of surface melting observed over Antarctica ice shelves using scatterometer data. *Antarct. Sci.*, 2015, **27**(4), 403–410; doi:10.1017/S0954102014000832.
19. Fricker, H., Coleman, R., Padman, L., Scambos, T., Bohlander, J. and Brunt, K., Mapping the grounding zone of the Amery Ice Shelf East Antarctica using InSAR, MODIS and ICESat. *Antarct. Sci.*, 2009, 515–532; doi:10.1017/S095410200999023X.

ACKNOWLEDGEMENT. We thank Shri Tapan Misra, Director SAC, ISRO for his support. Constant encouragement and guidance provided by Dr Raj Kumar, DD, EPSA and Dr A. S. Rajawat, GD, GHCAG/EPISA is deeply appreciated. We also thank Dr B. K. Jain, Principal, M.G. Science Institute, Ahmedabad and Dr Sushil Kumar Singh, Maya Suryawanshi and Naveen Tripathi for their valuable suggestions.

Received 29 November 2017; revised accepted 7 May 2018

doi: 10.18520/cs/v115/i9/1799-1804